



Efficient Counterselection for *Methylococcus capsulatus* (Bath) by Using a Mutated *pheS* Gene

Masahito Ishikawa,^a Sho Yokoe,^a Souichiro Kato,^b Katsutoshi Hori^a

^aDepartment of Biomolecular Engineering, Graduate School of Engineering, Nagoya University, Nagoya, Japan

^bBioproduction Research Institute, National Institute of Advanced Industrial Science and Technology, Sapporo, Japan

ABSTRACT *Methylococcus capsulatus* (Bath) is a representative gammaproteobacterial methanotroph that has been studied extensively in diverse research fields. The *sacB* gene, which encodes levansucrase, causing cell death in the presence of sucrose, is widely used as a counterselectable marker for disruption of a target gene in Gram-negative bacteria. However, *sacB* is not applicable to all Gram-negative bacteria, and its efficiency for the counterselection of *M. capsulatus* (Bath) is low. Here, we report the construction of an alternative counterselectable marker, *pheS*^{*}, by introduction of two point mutations (A306G and T252A) into the *pheS* gene from *M. capsulatus* (Bath), which encodes the α -subunit of phenylalanyl-tRNA synthetase. The transformant harboring *pheS*^{*} on an expression plasmid showed sensitivity to 10 mM *p*-chloro-phenylalanine, whereas the transformant harboring an empty plasmid showed no sensitivity, indicating the availability of *pheS*^{*} as a counterselectable marker in *M. capsulatus* (Bath). To validate the utility of the *pheS*^{*} marker in counterselection, we attempted to obtain an unmarked mutant of *xoxF*, a gene encoding the major subunit of Xox methanol dehydrogenase, which we failed to obtain by counterselection using the *sacB* marker. PCR, immunodetection using an anti-XoxF antiserum, and a cell growth assay in the absence of calcium demonstrated successful disruption of the *xoxF* gene in *M. capsulatus* (Bath). The difference in counterselection efficiencies of the markers indicated that *pheS*^{*} is more suitable than *sacB* for counterselection in *M. capsulatus* (Bath). This study provides a new genetic tool enabling efficient counterselection in *M. capsulatus* (Bath).

IMPORTANCE Methanotrophs have long been considered promising strains for biologically reducing methane from the environment and converting it into valuable products, because they can oxidize methane at ambient temperatures and pressures. Although several methodologies and tools for the genetic manipulation of methanotrophs have been developed, their mutagenic efficiency remains lower than that of tractable strains such as *Escherichia coli*. Therefore, further improvements are still desired. The significance of our study is that we increased the efficiency of counterselection in *M. capsulatus* (Bath) by employing *pheS*^{*}, which was newly constructed as a counterselectable marker. This will allow for the efficient production of gene-disrupted and gene-integrated mutants of *M. capsulatus* (Bath). We anticipate that this counterselection system will be utilized widely by the methanotroph research community, leading to improved productivity of methane-based bioproduction and new insights into methanotrophy.

KEYWORDS counterselection, *Methylococcus capsulatus*, methanotroph, *pheS*

The atmospheric concentration of the greenhouse gas methane is the second highest after carbon dioxide (CO₂), and methane has a global warming potential of 25 CO₂ equivalents (1). To mitigate global warming, it is important to reduce the levels

Received 31 July 2018 Accepted 22 September 2018

Accepted manuscript posted online 28 September 2018

Citation Ishikawa M, Yokoe S, Kato S, Hori K. 2018. Efficient counterselection for *Methylococcus capsulatus* (Bath) by using a mutated *pheS* gene. *Appl Environ Microbiol* 84:e01875-18. <https://doi.org/10.1128/AEM.01875-18>.

Editor Volker Müller, Goethe University Frankfurt am Main

Copyright © 2018 American Society for Microbiology. All Rights Reserved.

Address correspondence to Katsutoshi Hori, khor@chembio.nagoya-u.ac.jp.

of atmospheric methane. Environmental methane has attracted attention as a chemical feedstock because it exists as a main component of natural gas, shale gas, and biogas (2). Despite the high stability and low reactivity of the C-H bond in methane, methanotrophs can activate it through methane monooxygenase and utilize methane as a sole carbon and energy source. Therefore, methanotrophs have long been considered promising strains for biologically reducing methane and converting it into valuable products. Proteobacterial methanotrophs can be broadly divided into type I and type II, composed of gammaproteobacteria and alphaproteobacteria, respectively. Representatives of each type, namely, *Methylococcus capsulatus* (Bath) and *Methylosinus trichosporium* OB3b, have been studied extensively for methane-based bioproduction such as single-cell protein, polyhydroxybutyrate, vitamin, lipid, lactic acid, isoprene, succinic acid, and methanol production (3–6). Because the productivity of most of these processes remains low, efforts to improve them have been undertaken. Recent advances in metabolic engineering, synthetic biology, and genome-editing technologies have been anticipated to improve the productivity of methane-based bioproduction (7). Although genetic tools and electroporation techniques have been developed recently for both types of methanotrophs (8–12), the efficiency of genetic manipulation is still low compared to that for tractable host strains such as *Escherichia coli* (5). Further improvement of these tools and techniques is required for the efficient genetic manipulation of methanotrophs.

In counterselection for gene disruption in methanotrophs, the *sacB* gene is employed as the only available marker (8, 9, 12–16). Levansucrase, encoded by the *sacB* gene, converts sucrose into levan, which accumulates in the periplasmic space, thereby causing cell death in Gram-negative bacteria (17). However, *sacB* is not universal for all Gram-negative bacteria, resulting in the need for an alternative counterselectable marker (18). Mutated *pheS* (*pheS**), *rpsL*, *thyA*, and *tdk* are used frequently as alternative counterselectable markers (17, 19). The use of the counterselectable markers *rpsL*, *thyA*, and *tdk* depends on the host genotype; a host strain requires resistance to streptomycin for the use of *rpsL*, resistance to trimethoprim for the use of *thyA*, and resistance to a toxic nucleoside analog such as 5-fluoro-2'-deoxyuridine for the use of *tdk*. In contrast, *pheS** is a host genotype-independent counterselectable marker that requires no resistance in a host strain.

The *pheS* gene encodes the highly conserved α -subunit of phenylalanyl-tRNA synthetase. A counterselection system using *pheS** was first developed in *E. coli* (20). As PheS from *E. coli* with an A294G substitution shows low substrate specificity, PheS* incorporates *p*-chloro-phenylalanine (*p*-Cl-Phe) into proteins during translation, thereby causing cell death. Furthermore, Miyazaki recently reported that substitution of T251 in PheS from *E. coli* with alanine or serine increased the efficiency of counterselection (21). Although individual *pheS** genes have been constructed and used for counterselection in various bacteria (18, 22–25), counterselection using *pheS** has not been carried out in methanotrophs.

In this study, we aimed to develop an efficient gene disruption method for *M. capsulatus* (Bath) using *pheS** as a counterselectable marker. Then, we validated the efficiency of this novel method with the conventional *sacB* method by constructing disruptant strains targeting the *xoxF* gene (Table 1), a structural gene encoding one of the two isozymes of methanol dehydrogenase (MDH).

RESULTS

Low efficiency of counterselection using *sacB* in *M. capsulatus* (Bath). In this study, the *xoxF* gene, which encodes the structural protein MDH, was selected as a model gene to verify the efficiency of the gene disruption methods. Like other methanotrophs, *M. capsulatus* (Bath) possesses 2 different MDHs, namely, Mxa MDH and Xox MDH (26). Thus, inactivation of a single MDH is not lethal to methanotrophs. Moreover, the phenotype of an MDH mutant can be predicted because the MDHs are dependent on different metal elements for enzymatic activity (15, 27–30); Mxa MDH requires calcium, whereas Xox MDH requires a rare earth element. Because calcium ion

TABLE 1 Bacterial strains and plasmids used in this study

Strain or plasmid	Description ^a	Reference or source
<i>Methylococcus capsulatus</i> (Bath)		
Wild type	Wild-type strain	26
SC-SacB	Single-crossover mutant constructed by integration of pJQYS1 in flanking region of <i>xoxF</i> of <i>M. capsulatus</i> (Bath)	This study
SC-PheS*	Single-crossover mutant constructed by integration of pJQYS2 in flanking region of <i>xoxF</i> of <i>M. capsulatus</i> (Bath)	This study
$\Delta xoxF$	Unmarked mutant of <i>xoxF</i> (MCA0299)	This study
Bath (empty)	Transformant of <i>M. capsulatus</i> (Bath) harboring pJN105 (vector control)	This study
Bath (pPheS*)	Transformant of <i>M. capsulatus</i> (Bath) harboring pPheS*	This study
<i>Escherichia coli</i>		
XL10-Gold	Host for routine cloning	Agilent
WM6026	Donor strain for conjugation	46
Plasmids		
pJQ200sk	Suicide plasmid; Gm ^r , SacB	45
pUC57- <i>pheS</i> *	pUC57 harboring <i>pheS</i> *	This study
pJQY3	Suicide plasmid produced by substitution of <i>sacB</i> in pJQ200sk with <i>pheS</i> *	This study
pJQYS1	DNA fragment containing upstream and downstream regions of <i>xoxF</i> ligated into BamHI site of pJQ200sk	This study
pJQYS2	DNA fragment containing upstream and downstream regions of <i>xoxF</i> ligated into BamHI site of pJQY3	This study
pJN105	Broad-host-range plasmid; Gm ^r , <i>araC</i> -P _{BAD} promoter	44
pPheS*	pJN105 carrying <i>pheS</i> * derived from <i>M. capsulatus</i> (Bath) under control of <i>araC</i> -P _{BAD} promoter	This study

^aGm^r, gentamicin resistance.

is found in the crystal structure of Mxa MDH from *M. capsulatus* (Bath) (31), its $\Delta xoxF$ mutant was assumed to show a calcium-dependent phenotype.

First, we attempted to construct a mutant of *xoxF* with a typical plasmid-based method, using the *sacB* gene as a counterselectable marker (Fig. 1). To prepare the suicide plasmid pJQYS1, the upstream and downstream regions of the *xoxF* gene were cloned into pJQ200sk, which is the same plasmid as used previously for counterselection in *M. capsulatus* (Bath) (13). Plasmid integration into the target site was confirmed by PCR using the Scr-F and Scr-R primers in a single-crossover mutant (SC-SacB) grown on a gentamicin plate (Fig. 2A). The Scr-F and Scr-R primers anneal to the outside and the inside, respectively, of the flanking regions of the *xoxF* gene used as homologous sites for recombination (Table 2). Although 1,897-bp and 10,655-bp DNA bands were expected to appear, the shorter fragment was amplified predominantly. The SC-SacB mutant was then plated on a sucrose plate for counterselection. From the resultant colonies on the sucrose plate, we attempted to select double-crossover mutants by PCR using the primers Scr-F and Scr-R2, but we were unable to obtain an expected mutant. To confirm the emergence of double-crossover mutants, colonies grown on the sucrose plate were transferred to a gentamicin plate. All of the tested colonies showed resistance to gentamicin, indicating that no double-crossover mutants were generated (Table 3). This low efficiency of counterselection suggested that selection pressure from sucrose was not lethal to the SC-SacB mutant. To confirm selection pressure from sucrose in the SC-SacB mutant, serial dilutions of the cell suspension were spotted on a sucrose plate (Fig. 2B). There was no clear difference in cell growth between wild-type and SC-SacB mutant colonies. When the SC-SacB mutant was cultivated on a sucrose plate, we observed a difference in appearance between wild-type and SC-SacB mutant colonies; SC-SacB colonies appeared to be lysed (Fig. 2C). Because the sucrose concentration was assumed not to be sufficiently high enough to cause cell death of the SC-SacB mutant, the concentration was increased to 10% (wt/vol). However, this high sucrose concentration inhibited the growth of wild-type colonies (data not shown). These results implied that SacB was unlikely to function effectively as a counterselectable marker in the SC-SacB mutant.

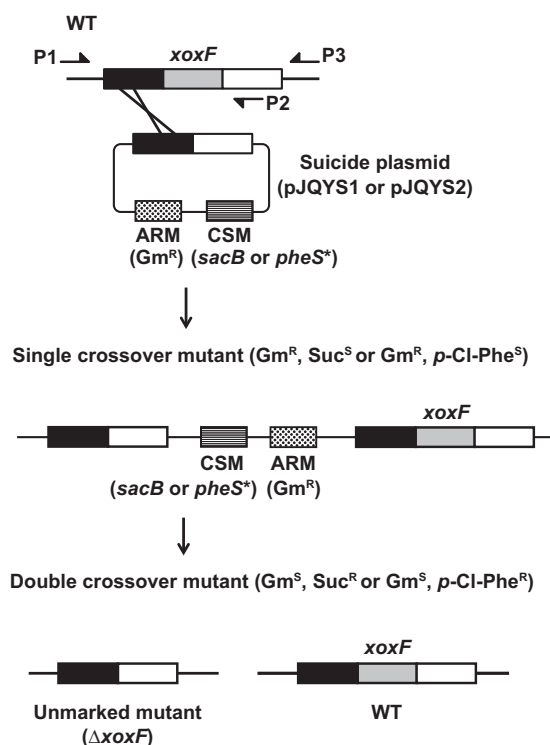


FIG 1 Schematic representation of plasmid-based counterselection. The suicide plasmids, antibiotic resistance marker (ARM), and counterselectable marker (CRM) used in this study are indicated in parentheses. *Gm^r*, gentamicin resistance gene. Half arrows indicate primers (P1, Scr-F; P2, Scr-R; P3, Scr-F2). The nucleotide sequences of these primers are shown in Table 2. Suc, sucrose; WT, wild type.

Construction of a *pheS** marker for counterselection in *M. capsulatus* (Bath).

Instead of the *sacB* marker, we attempted to employ a *pheS** marker, which has been established as a counterselectable marker in various bacteria (18, 22–25), for counterselection in *M. capsulatus* (Bath). The amino acid sequence of PheS from *M. capsulatus* (Bath) was aligned with those from *E. coli* and other representative methanotrophs (Fig. 3). PheS from *M. capsulatus* (Bath) possesses conserved alanine (A306) and tyrosine (T252) residues, corresponding to A294 and T251, respectively, in PheS from *E. coli*. To construct *PheS** available for counterselection in *M. capsulatus* (Bath), we added two point mutations (A306G and T252A) to PheS from *M. capsulatus* (Bath). In the case of counterselection using *pheS**, there is concern regarding homologous recombination between the *pheS** cassette and the chromosomal copy of *pheS*, which reduces the efficiency of counterselection. Xie et al. reported that silent mutations downstream of the *pheS** point mutation site could prevent such homologous recombination (23). Based on that report, we introduced silent mutations into *pheS** from *M. capsulatus* (Bath) when constructing it by artificial gene synthesis (see Fig. S1 in the supplemental material).

To determine whether the constructed *pheS** caused cell death of *M. capsulatus* (Bath) in the presence of *p*-Cl-Phe, we examined the *p*-Cl-Phe sensitivity of the transformant, Bath (p*PheS**), harboring the *pheS** gene under the control of the arabinose-inducible promoter on the expression plasmid. Bath (p*PheS**) and Bath (empty), a vector control, were spotted onto nitrate mineral salt (NMS) plates containing different concentrations of *p*-Cl-Phe (Fig. 4). In the presence of arabinose (0.5% [wt/vol]), Bath (p*PheS**) did not show impaired growth on the 5 mM *p*-Cl-Phe plate but growth inhibition of Bath (p*PheS**) was observed on NMS plates containing >10 mM *p*-Cl-Phe, implying that *pheS** functions as a counterselectable marker in *M. capsulatus* (Bath). The cell growth of Bath (p*PheS**) was highly repressed on the 15 mM *p*-Cl-Phe plate, but Bath (empty) also showed growth inhibition. In the absence of arabinose, Bath (p*PheS**)

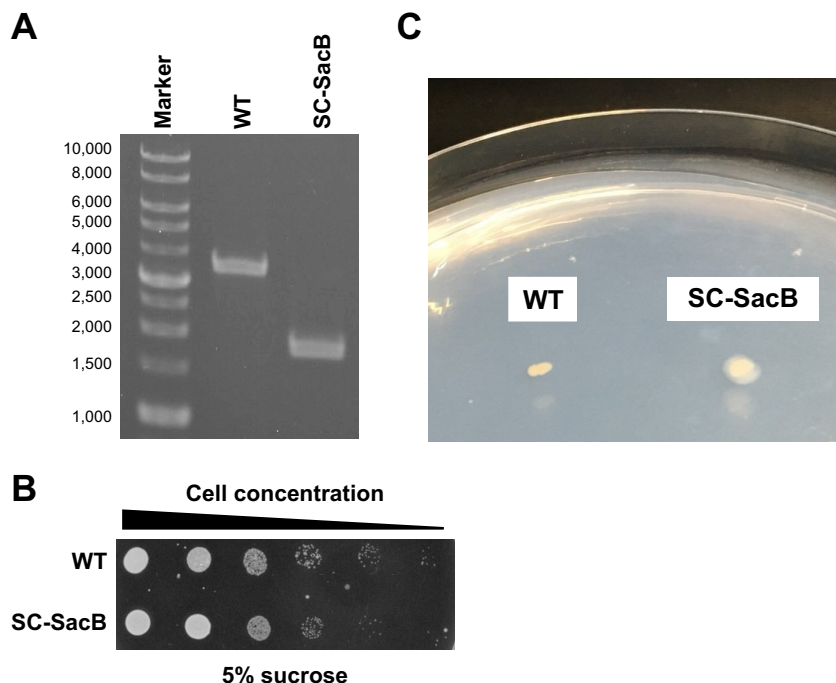


FIG 2 Counterselection using *sacB* in *Methylococcus capsulatus* (Bath). (A) PCR confirmation of plasmid integration. PCR was performed using the primers Scr-F and Scr-R. The nucleotide sequences of these primers are shown in Table 2. From the genome sequence information for *M. capsulatus* (Bath), the lengths of PCR amplicons from the wild type (WT) and SC-SacB are expected to be 3,633 bp and 1,897 bp plus 10,655 bp, respectively. The PCR amplicon from SC-SacB indicates plasmid integration into the flanking chromosomal region of *xoxF*. (B) Sucrose sensitivity of a plasmid-integrated mutant of *M. capsulatus*. Cell suspensions of the wild type and the plasmid-integrated mutant (SC-SacB) were serially diluted 1:10. Each serial dilution was spotted onto an NMS agar plate containing 5% sucrose. (C) Different appearances of wild-type and SC-SacB colonies on an NMS agar plate containing 5% sucrose.

showed resistance to *p*-Cl-Phe due to the lack of *pheS** expression (Fig. S2). These results suggest that the *pheS** system can work as a counterselectable marker in *M. capsulatus* (Bath) and 10 mM *p*-Cl-Phe should be used for counterselection.

Validation of the utility of the constructed *pheS as a counterselectable marker in *M. capsulatus* (Bath).** To validate the utility of the constructed *pheS** gene, we attempted to construct a *xoxF* mutant, which we were unable to generate by counterselection using *sacB*. To prepare the suicide plasmid pJQYS2, the *sacB* gene on the pJQ200sk plasmid was substituted with the constructed *pheS** gene, and then the flanking region of the *xoxF* gene was cloned into it. On this new suicide plasmid, the J23119 promoter was employed to drive constitutive expression of the *pheS** gene.

TABLE 2 Primers used in this study

Primer name	Sequence (5' to 3')
xoxF-upstF	CGAATTCCTGCAGCCCGGGGATCCAGTTCATGCTTTCCTCG
xoxF-upstR	CCAGACCTTCAACTTGCATGAGCCAGC
xoxF-dwstF	ATCGCAAGTTGAAGGTCTGGGTGCGGTG
xoxF-dwstR	CGGCCGCTCTAGAACTAGTGATCCGGCTTGTTGTGATAGACCAG
PheS-F	CTAGCTAGAGGATCGATCCTCTGCAGTTGACAGCTAGC
PheS-R	TTGCGTTTTTACAGCTGTCGTCAGAAGGGTTTGAAGT
iPCR-pJQR	AGGATCGATCCTCTAGCTAGA
iPCR-pJQF	CGACAGCTGTAAAAACGAAAAGAAAATGCCGA
pPheS-F	ACCCGTTTTTTGGGCTAGCCTGCAGTTGACAGCTAGC
pPheS-R	GTGGATCCCCGGGCTGCAGTCAGAAGGGTTTGAAGT
Scr-F	GTTGCAAGACCGTTGAGATAGCGTTCCTCG
Scr-R	AGCCGTGCAACATGGCGATC
Scr-R2	CAGCGGGACGTGATATTCTCAGCAGAGC

TABLE 3 Comparison of the mutagenic efficiency of different counterselectable markers

Marker	Selection ^a	No. of mutants ^b		Efficiency (%)
		Double-crossover mutant	Unexpected mutant	
<i>sacB</i>	Gm, Suc	0 (Gm ^s , Suc ^r)	60 (Gm ^r , Suc ^r)	0
<i>pheS*</i>	Gm, Cl-Phe	19 (Gm ^s , Cl-Phe ^r)	41 (Gm ^r , Cl-Phe ^r)	31.7

^aGm, gentamicin; Suc, sucrose; Cl-Phe, *p*-chloro-phenylalanine.

^bSixty colonies were randomly selected to test for resistance (r) or sensitivity (s) to each chemical.

Plasmid integration into the target site was confirmed by PCR using Scr-F and Scr-R in the single-crossover mutant (SC-PheS*) grown on a gentamicin plate (Fig. 5A). Although 1,897-bp and 9,872-bp DNA bands were expected to appear, the shorter fragment was amplified predominantly, as when the SC-SacB mutant was examined for plasmid integration. As expected, SC-PheS* showed growth inhibition in the presence of 10 mM *p*-Cl-Phe (Fig. 5B). To select double-crossover mutants, a cell suspension of SC-PheS was spread on an NMS plate containing 10 mM *p*-Cl-Phe. Colonies grown on the *p*-Cl-Phe-plate were transferred to a gentamicin plate in order to examine whether double-crossover mutants were obtained. Although no gentamicin-sensitive colonies were obtained by counterselection using *sacB*, 19 of the 60 tested colonies showed sensitivity to gentamicin, indicating the emergence of double-crossover mutants (Table 3). Alteration of the marker drastically increased the efficiency of counterselection. Some of the gentamicin-sensitive mutants possibly reverted to the wild-type genotype (Fig. 1). Unmarked $\Delta xoxF$ mutants were selected from the gentamicin-sensitive colonies by PCR using the primers Scr-F and Scr-R2, which anneal to the outside of the flanking regions of the *xoxF* gene used as homologous sites. The length of the PCR amplicon from $\Delta xoxF$ mutant colonies was shorter than that from wild-type colonies (Fig. 5C). Furthermore, immunodetection using anti-XoxF and anti-MxaF antisera demonstrated the lack of *xoxF* expression and the presence of *mxoF* expression in the $\Delta xoxF$ mutant (Fig. 5D). These results indicate successful excision of the *xoxF* gene together with the region derived from the integrated plasmid.

We confirmed the physiological modification of the $\Delta xoxF$ mutant by growth experiments. Mxa MDH and Xox MDH require calcium and a rare earth element (such as cerium), respectively, for enzymatic activity (15, 27–30). When Xox MDH is inactive, *M. capsulatus* (Bath) depends on Mxa MDH for methanol oxidation. Thus, the $\Delta xoxF$ mutant was assumed not to grow in the absence of calcium. After the wild type and the $\Delta xoxF$ mutant of *M. capsulatus* (Bath) were cultivated in the presence of calcium, the cells were transferred to NMS medium containing either 0 μ M calcium and 20 μ M cerium or 20 μ M calcium and 20 μ M cerium. As expected, the $\Delta xoxF$ mutant barely grew in the absence of calcium, whereas wild-type *M. capsulatus* (Bath) grew regardless of the presence or absence of calcium (Fig. 6). This calcium-dependent cell growth indicates the successful disruption of *xoxF* in *M. capsulatus* (Bath).

DISCUSSION

In this study, we constructed a counterselectable *pheS** marker by introducing two point mutations (A306G and T252A) into the *pheS* gene from *M. capsulatus* (Bath). Unlike other counterselectable markers, the *pheS** marker has a risk of homologous

<i>Escherichia coli</i>	247	YFPFTEPSAEVDV	MGKNGK	- - - - -	WLEVLGCGMVHPNVLRNVG	I	DPEVYSGFA	FGMGMER	301			
<i>Methylococcus capsulatus</i> (Bath)	248	YFPFTEPSAEVDI	ECV	I	CDGRGCRVCKHSGWLEVMGCGMI	HPRVFEAVG	I	DPERYSGFA	FGLGVER	313		
<i>Methylomonas</i> sp. LW13	248	YFPFTEPSAEFDV	SCVMCDGKGRVCKQTGWLEVGCGMI	HPEVFKSVG	I	DNQVYSGFA	F	FGTGV	313			
<i>Methylobacter tundripaludum</i> 21/22	248	YFPFTEPSAEVDI	ECVMCGGQGRVCSHTGWLEVMGCGMI	HPEVFKAVN	I	DSETYSGFA	FGMGVER	313				
<i>Methylocrobinium buryatense</i> 5G	248	YFPFTEPSAEVDI	ECVMCEGKGRVCGHTGWLEVMGCGMI	HPEVFKSVG	I	SNEMYSGFA	FGMGVER	313				
<i>Methylosinus trichosporium</i> OB3b	255	FFPFTEPSAEVDV	QCRRQGGD	- I	RFEGEDVME	I	LGCGMVHPNVLRNCG	LD	DPDKYQGF	FGLGIDR	319	
<i>Methylocystis</i> sp. SC2	254	FFPFTEPSMEVDV	QCRRQGGG	- I	RFEGEDVME	I	LGCGMVHPNVLRNCG	I	DPDRYQGF	FGVGVDR	318	
<i>Methylocella silvestris</i> BL2	255	YFPFTEPSMEVDV	QCSRKGDG	- I	RFEGESDWLE	I	LGCGMVHPNVLRNCG	LDPE	I	FQGFAG	IGIDR	319

FIG 3 Sequence alignment of PheS orthologs derived from *Escherichia coli* and representative methanotrophs. Red boxes indicate the conserved residues, corresponding to tyrosine at position 251 and alanine at position 294 in *E. coli*. The T251A and A294G substitutions are known to reduce the substrate specificity of PheS and allow incorporation of *p*-Cl-Phe into proteins during translation, thereby causing cell death.

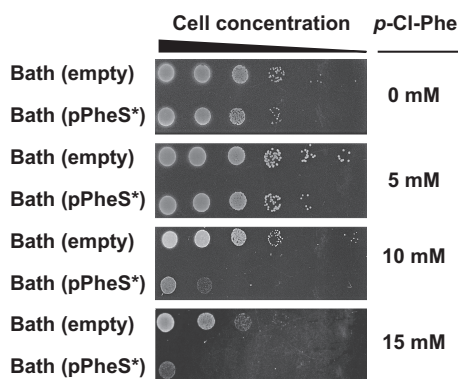


FIG 4 *p*-Cl-Phe sensitivity of *Methylococcus capsulatus* (Bath) transformants. Cell cultures of transformants harboring the empty vector, i.e., Bath (empty), and harboring pPheS*, i.e., Bath (pPheS*), were serially diluted 1:10. Each serial dilution was spotted onto agar plates containing *p*-Cl-Phe at different concentrations and 0.5% (wt/vol) arabinose.

recombination with the chromosomal copy of *pheS*, which reduces the efficiency of counterselection. To avoid this, we added silent mutations downstream of the *pheS** point mutation site, following the report by Xie et al. (23) (see Fig. S1 in the supplemental material). As a result, the constructed *pheS** marker enabled more efficient counterselection than did the conventional *sacB* marker. In addition, we clarified the inefficiency of counterselection using *sacB* in *M. capsulatus* (Bath). Although the *sacB* gene is the most commonly used counterselectable marker for Gram-negative bacteria, only a few reports have described application of the *sacB* method to produce disruptants of *M. capsulatus* (Bath) (13, 14). This is probably due to the inefficiency of the *sacB* system in *M. capsulatus* (Bath), as observed in this study. From the difference in appearance between wild-type and SC-SacB mutant colonies (Fig. 2C), we assumed that SacB functioned in the SC-SacB mutant, resulting in the accumulation of levan in the periplasm, but the level of levan accumulation was not sufficient to cause cell death for efficient counterselection. This implies that counterselection using *sacB* in *M. capsulatus* (Bath) would require screening of many sucrose-resistant colonies in order to obtain a double-crossover mutant. In contrast, counterselection using *pheS** in *M. capsulatus* (Bath) enables a double-crossover mutant to be obtained from fewer *p*-Cl-Phe-resistant colonies. The results of this study demonstrate that *pheS** is more suitable than *sacB* as a counterselectable marker in *M. capsulatus* (Bath). *M. capsulatus* (Bath) has been studied extensively not only in methane-based bioproduction (4–6) but also in a broad range of fields, including copper-dependent physiological processes (32–37), outer membrane proteins associated with extracellular electron transfer (32, 37, 38), and probiotics for treatment of mammalian diseases (39, 40). The establishment of an efficient counterselection system using *pheS** will facilitate such studies.

The *pheS** method described here can be applicable to other methanotrophs, in addition to *M. capsulatus* (Bath). The alignment shown in Fig. 3 displays the conservation of 2 important residues for the construction of a counterselectable marker in other methanotrophs. Pairwise sequence alignment using the EMBOSS Needle program revealed that PheS from *M. capsulatus* (Bath) shares a high level of sequence similarity with orthologs from other methanotrophs, especially representative type I methanotrophs whose genetic manipulation has been reported (Table 4) (5). PheS* can be used as a counterselectable marker even in nonnative host strains when PheS* shares a high level of sequence similarity with a host-derived PheS. For instance, Argov et al. employed the PheS* marker derived from *Bacillus subtilis* for counterselection in *Listeria monocytogenes* (22); pairwise sequence alignment showed 83.1% similarity (69.4% identity) between PheS from *B. subtilis* and that from *L. monocytogenes*. Due to the high levels of sequence similarity/identity, the *pheS** gene constructed in this study might be available for a wide range of type I methanotrophs, including *Methylomicrobium*

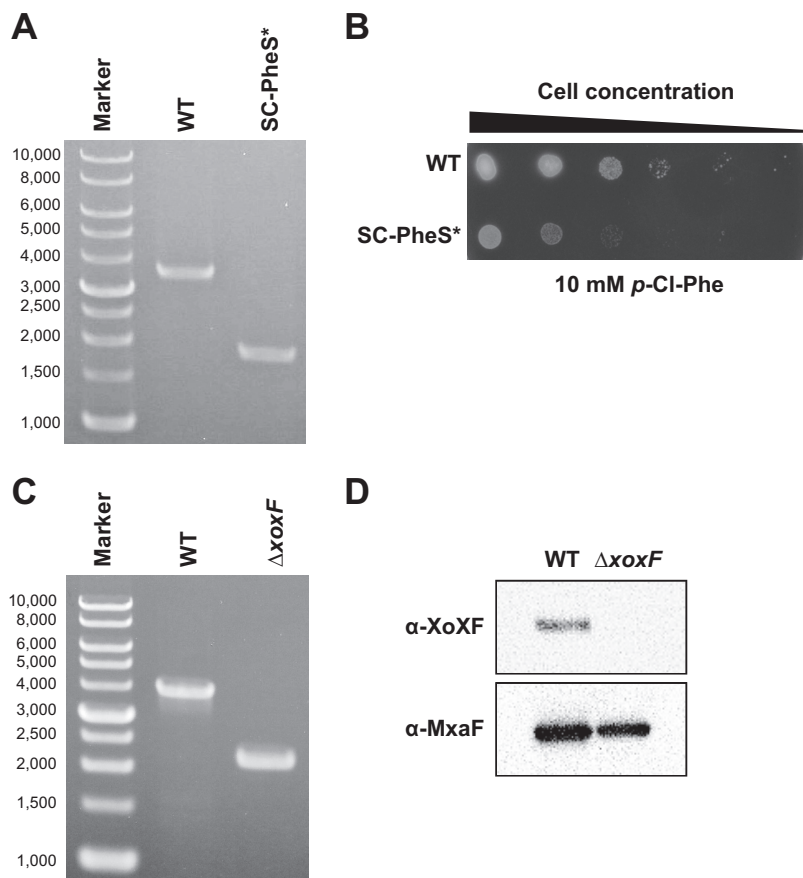


FIG 5 Counterselection using *pheS** in *Methylococcus capsulatus* (Bath). (A) PCR confirmation of plasmid integration. PCR was performed using the primers Scr-F and Scr-R. The nucleotide sequences of these primers are shown in Table 2. From the genome sequence information for *M. capsulatus* (Bath), the lengths of PCR amplicons from the wild type (WT) and SC-PheS* are expected to be 3,633 bp and 1,897 bp plus 9,872 bp, respectively. The PCR amplicon from SC-PheS* indicates plasmid integration into the flanking chromosomal region of *xoxF*. (B) *p*-Cl-Phe sensitivity of SC-PheS*. Cell suspensions of the wild type and SC-PheS* were serially diluted 1:10. Each serial dilution was spotted onto an NMS agar plate containing 10 mM *p*-Cl-Phe. (C) PCR confirmation of *xoxF* disruption. PCR was performed using the primers Scr-F and Scr-R2. The nucleotide sequences of these primers are shown in Table 2. From the genome sequence information for *M. capsulatus* (Bath), the lengths of PCR amplicons from the wild type and the $\Delta xoxF$ mutant are expected to be 3,989 bp and 2,253 bp, respectively. (D) Immunodetection of XoxF and MxaF using specific antisera.

buryatense 5GB1C, *Methylomonas* sp. strain LW13, and *Methylobacter tundripaludum* 21/22.

MATERIALS AND METHODS

Bacterial strains, plasmids, and growth conditions. The bacterial strains used in this study are listed in Table 1. *M. capsulatus* (Bath) and its derivative mutants were grown for 3 to 4 days at 42°C on NMS medium (41) supplemented with 1 μ M CuSO₄ and 20% (vol/vol) methane, with shaking. For the calcium dependency test, *M. capsulatus* (Bath) and its derivative mutants were cultured in a calcium-free inorganic medium composed of 5 mM NaNO₃, 2 mM KH₂PO₄, 1 mM MgCl₂, 0.1 mM Na₂SO₄, 20 mM HEPES, 10 μ M CuCl₂, and 10 ml/liter each of a trace element solution (CaCl₂ was omitted) and a vitamin solution (42). Methane (20% [vol/vol]) and CaCl₂ and/or CeCl₂ (final concentration of 20 μ M each) were supplemented after autoclaving. *E. coli* strains were grown at 37°C in Luria-Bertani medium, with shaking. Gentamicin (10 μ g/ml) and 600 μ M 2,6-diaminopimelic acid (DAP) were added to the medium when required. Arabinose was added to a final concentration of 0.5% (wt/vol) for gene expression under the control of the P_{BAD} promoter. Transformation of *M. capsulatus* (Bath) with a broad-host-range plasmid, such as pJN105 or pPheS*, was performed following the method described by Ishikawa et al. (43).

Sequence analysis. Multiple sequence alignments were made using ClustalW (<http://www.clustal.org/clustal2>) and Jalview (<http://www.jalview.org>). Pairwise sequence alignment was performed using the EMBOSS Needle program (http://www.ebi.ac.uk/Tools/psa/emboss_needle) to calculate identity and similarity values.

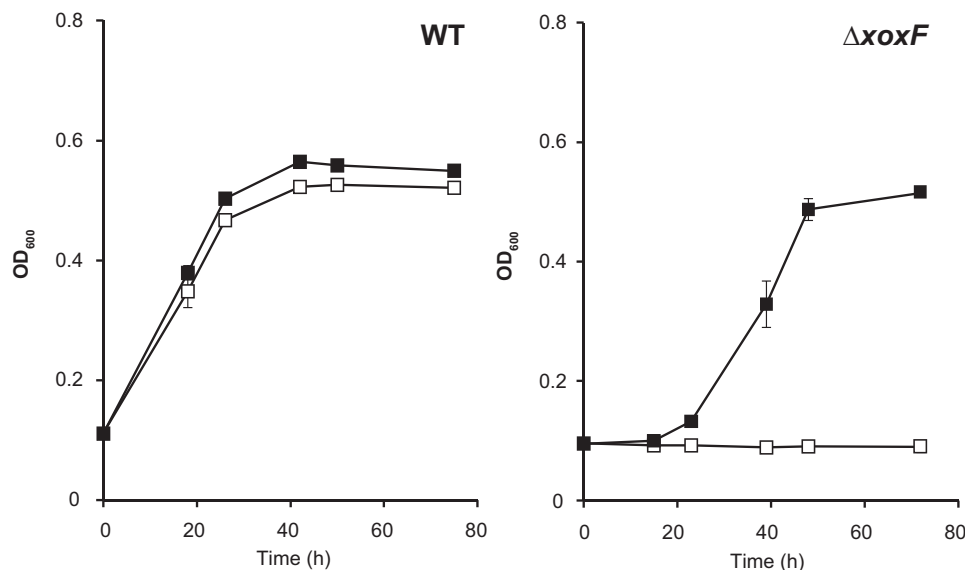


FIG 6 Growth of the wild type (WT) and the $\Delta xoxF$ mutant in NMS medium containing either 0 μM calcium and 20 μM cerium or 20 μM calcium and 20 μM cerium. Closed squares represent cell growth in NMS medium containing 20 μM calcium and 20 μM cerium; open squares represent cell growth in NMS medium containing 0 μM calcium and 20 μM cerium. The experiments were conducted in triplicate. Error bars indicate standard deviations ($n = 3$). OD₆₀₀, optical density at 600 nm.

Plasmid construction. The primers used in this study are listed in Table 2. The *pheS** gene cassette, including a J23119 promoter, ribosome binding site (RBS), and mutated *pheS* (*pheS**) gene, was artificially synthesized and cloned into pUC57, generating pUC57-*pheS** (Genewiz, Saitama, Japan); the RBS originated from the wild-type *pheS* of *M. capsulatus* (Bath). For the construction of a *pheS** expression plasmid, a *pheS** gene cassette without the J23119 promoter was amplified from pUC57-*pheS** by PCR using the primer set pPheS-F/pPheS-R and was cloned into the EcoRI site of pJN105 (44) with the NEBuilder HiFi DNA assembly system (New England BioLabs), generating pPheS*. For the construction of a suicide plasmid carrying *pheS** as a counterselectable marker, a *pheS** gene fragment amplified from pUC57-*pheS** by PCR using the primer set PheS-F/PheS-R and a plasmid backbone amplified from pJQ200sk (45) by inverse PCR using the primer set iPCR-pJQF/iPCR-pJQR were ligated by the NEBuilder HiFi DNA assembly system, generating pJQY3.

Construction of a deletion mutant of *xoxF* in *M. capsulatus* (Bath). To obtain a deletion mutant of the *xoxF* gene in *M. capsulatus* (Bath), DNA fragments including the 1-kb upstream and 1-kb downstream regions of *xoxF* were cloned into the BamHI sites of pJQ200sk and pJQY3, generating pJQY51 and pJQY52, respectively; the primer sets *xoxF*-upstF/*xoxF*-upstR and *xoxF*-dwstF/*xoxF*-dwstR and the NEBuilder HiFi DNA assembly system were used. *M. capsulatus* (Bath) was mated for 24 h at 37°C with *E. coli* WMM6026 (46) harboring pJQY51 or pJQY52, on an NMS agar plate containing 600 μM DAP and supplied with methane vapor. The cells were collected in 500 μl NMS medium, plated on an NMS agar plate containing gentamicin (10 $\mu\text{g}/\text{ml}$), supplied with methane vapor, and incubated at 37°C until colonies were generated. Chromosomal integration of the plasmid in the resulting colonies was confirmed by PCR using the primer set Scr-F/Scr-R; thus, the single-crossover mutants SC-SacB and SC-PheS were obtained. These single-crossover mutants were plated on an NMS agar plate containing 5% sucrose or 10 mM *p*-Cl-Phe and were incubated at 37°C, supplied with methane vapor. The resultant colonies, which were resistant to sucrose or *p*-Cl-Phe, were transferred, using toothpicks, to a gentamicin-NMS agar plate to select double-crossover mutants that showed sensitivity to gentamicin.

TABLE 4 Similarity and identity of PheS in representative methanotrophs

Methanotroph	Type	Similarity (%) ^a	Identity (%) ^a	GenBank accession no.
<i>Methylobacter tundripaludum</i> 21/22	I	83.7	73.9	WP_031437875.1
<i>Methylomicrobium buryatense</i> 5G	I	84.8	72.1	WP_017840103.1
<i>Methylomonas</i> sp. LW13	I	82.4	69.5	WP_033158015.1
<i>Methylocella silvestris</i> BL2	II	60.9	47	ACK50391.1
<i>Methylocystis</i> sp. SC2	II	61.6	47.4	CCJ08353.1
<i>Methylosinus trichosporium</i> OB3b	II	65.0	50.1	ATQ70420.1

^aSimilarity and identity with PheS of *Methylococcus capsulatus* (Bath) were calculated with the Needle program.

Immunodetection. Anti-XoxF and anti-MxaF antisera were generated against synthesized peptides corresponding to residues 398 to 411 of XoxF and residues 25 to 38 of MxaF, respectively. Whole-cell lysates of *M. capsulatus* (Bath) and its Δ xoxF mutant were separated on a 10% (wt/vol) acrylamide gel and transferred to a polyvinylidene fluoride membrane following general protocols. The blotted membrane was blocked for 1 h at room temperature with a 5% (wt/vol) skim milk solution and then was treated for 1 h at room temperature with the anti-XoxF or anti-MxaF antiserum at a 1:2,000 dilution in phosphate-buffered saline (PBS) containing 0.05% (vol/vol) Tween 20 (Calbiochem) (PBS-T). XoxF and MxaF on the membrane were detected with a horseradish peroxidase-conjugated anti-rabbit IgG antibody (GE Healthcare), at a 1:10,000 dilution in PBS-T, and were visualized using Chemi-Lumi One Super (Nacalai Tesque).

SUPPLEMENTAL MATERIAL

Supplemental material for this article may be found at <https://doi.org/10.1128/AEM.01875-18>.

SUPPLEMENTAL FILE 1, PDF file, 0.2 MB.

ACKNOWLEDGMENTS

This work was supported by the Advanced Low Carbon Technology Research and Development Program of the Japan Science and Technology Agency.

We thank Motoko Takashino and Eriko Kawamoto for technical assistance.

REFERENCES

- Forster P, Ramaswamy V, Artaxo P, Bernsten T, Betts R, Fahey DW, Haywood J, Lean J, Lowe DC, Myhre G, Nganga J, Prinn R, Raga G, Schultz M, Van Dorland R. 2007. Changes in atmospheric constituents and in radiative forcing, p 129–234. In Solomon S, Qin D, Manning M, Chen Z, Marquis M, Averyt KB, Tignor M, Miller H (ed), *Climate change 2007: the physical science basis: contribution of working group I to the fourth assessment report of the Intergovernmental Panel on Climate Change*. Cambridge University Press, Cambridge, United Kingdom.
- Fei Q, Guarnieri MT, Tao L, Laurens LM, Dowe N, Pienkos PT. 2014. Bioconversion of natural gas to liquid fuel: opportunities and challenges. *Biotechnol Adv* 32:596–614. <https://doi.org/10.1016/j.biotechadv.2014.03.011>.
- Strong PJ, Kalyuzhnaya M, Silverman J, Clarke WP. 2016. A methanotroph-based biorefinery: potential scenarios for generating multiple products from a single fermentation. *Bioresour Technol* 215: 314–323. <https://doi.org/10.1016/j.biortech.2016.04.099>.
- Hwang IY, Nguyen AD, Nguyen TT, Nguyen LT, Lee OK, Lee EY. 2018. Biological conversion of methane to chemicals and fuels: technical challenges and issues. *Appl Microbiol Biotechnol* 102:3071–3080. <https://doi.org/10.1007/s00253-018-8842-7>.
- Lee OK, Hur DH, Nguyen DTN, Lee EY. 2016. Metabolic engineering of methanotrophs and its application to production of chemicals and biofuels from methane. *Biofuel Bioprod Biorefin* 10:848–863. <https://doi.org/10.1002/bbb.1678>.
- Cantera S, Munoz R, Lebrero R, Lopez JC, Rodriguez Y, Garcia-Encina PA. 2018. Technologies for the bioconversion of methane into more valuable products. *Curr Opin Biotechnol* 50:128–135. <https://doi.org/10.1016/j.copbio.2017.12.021>.
- Clomburg JM, Crumbley AM, Gonzalez R. 2017. Industrial biomanufacturing: the future of chemical production. *Science* 355:aag0804. <https://doi.org/10.1126/science.aag0804>.
- Yan X, Chu F, Puri AW, Fu Y, Lidstrom ME. 2016. Electroporation-based genetic manipulation in type I methanotrophs. *Appl Environ Microbiol* 82:2062–2069. <https://doi.org/10.1128/AEM.03724-15>.
- Puri AW, Owen S, Chu F, Chavkin T, Beck DA, Kalyuzhnaya MG, Lidstrom ME. 2015. Genetic tools for the industrially promising methanotroph *Methylobacterium buryatense*. *Appl Environ Microbiol* 81:1775–1781. <https://doi.org/10.1128/AEM.03795-14>.
- Crombie A, Murrell JC. 2011. Development of a system for genetic manipulation of the facultative methanotroph *Methylocella silvestris* BL2. *Methods Enzymol* 495:119–133. <https://doi.org/10.1016/B978-0-12-386905-0.00008-5>.
- Baani M, Liesack W. 2008. Two isozymes of particulate methane monooxygenase with different methane oxidation kinetics are found in *Methylocystis* sp. strain SC2. *Proc Natl Acad Sci U S A* 105:10203–10208. <https://doi.org/10.1073/pnas.0702643105>.
- Sharpe PL, Dicosimo D, Bosak MD, Knoke K, Tao L, Cheng Q, Ye RW. 2007. Use of transposon promoter-probe vectors in the metabolic engineering of the obligate methanotroph *Methylobacterium* sp. strain 16a for enhanced C40 carotenoid synthesis. *Appl Environ Microbiol* 73:1721–1728. <https://doi.org/10.1128/AEM.01332-06>.
- Welander PV, Summons RE. 2012. Discovery, taxonomic distribution, and phenotypic characterization of a gene required for 3-methylhopanoid production. *Proc Natl Acad Sci U S A* 109:12905–12910. <https://doi.org/10.1073/pnas.1208255109>.
- Csaki R, Bodrossy L, Klem J, Murrell JC, Kovacs KL. 2003. Genes involved in the copper-dependent regulation of soluble methane monooxygenase of *Methylobacterium capsulatus* (Bath): cloning, sequencing and mutational analysis. *Microbiology* 149:1785–1795. <https://doi.org/10.1099/mic.0.26061-0>.
- Farhan UI Haque M, Gu W, DiSpirito AA, Semrau JD. 2015. Marker exchange mutagenesis of *mxoF*, encoding the large subunit of the Mxa methanol dehydrogenase, in *Methylobacterium trichosporium* OB3b. *Appl Environ Microbiol* 82:1549–1555. <https://doi.org/10.1128/AEM.03615-15>.
- Nguyen AD, Hwang IY, Lee OK, Kim D, Kalyuzhnaya MG, Mariyana R, Hadiyati S, Kim MS, Lee EY. 2018. Systematic metabolic engineering of *Methylobacterium alcaliphilum* 20Z for 2,3-butanediol production from methane. *Metab Eng* 47:323–333. <https://doi.org/10.1016/j.ymben.2018.04.010>.
- Reyrat JM, Pelicic V, Gicquel B, Rappuoli R. 1998. Counterselectable markers: untapped tools for bacterial genetics and pathogenesis. *Infect Immun* 66:4011–4017.
- Barrett AR, Kang Y, Inamasu KS, Son MS, Vukovich JM, Hoang TT. 2008. Genetic tools for allelic replacement in *Burkholderia* species. *Appl Environ Microbiol* 74:4498–4508. <https://doi.org/10.1128/AEM.00531-08>.
- Metzgar D, Bacher JM, Pezo V, Reader J, Doring V, Schimmel P, Marliere P, de Crecy-Lagard V. 2004. *Acinetobacter* sp. ADP1: an ideal model organism for genetic analysis and genome engineering. *Nucleic Acids Res* 32:5780–5790.
- Kast P. 1994. pKSS: a second-generation general purpose cloning vector for efficient positive selection of recombinant clones. *Gene* 138: 109–114. [https://doi.org/10.1016/0378-1119\(94\)90790-0](https://doi.org/10.1016/0378-1119(94)90790-0).
- Miyazaki K. 2015. Molecular engineering of a PheS counterselection marker for improved operating efficiency in *Escherichia coli*. *Biotechniques* 58:86–88. <https://doi.org/10.2144/000114257>.
- Argov T, Rabinovich L, Sigal N, Herskovits AA. 2017. An effective counterselection system for *Listeria monocytogenes* and its use to characterize the monocin genomic region of strain 10403S. *Appl Environ Microbiol* 83:e02927-16. <https://doi.org/10.1128/AEM.02927-16>.
- Xie Z, Okinaga T, Qi F, Zhang Z, Merritt J. 2011. Cloning-independent and counterselectable markerless mutagenesis system in *Streptococ-*

- cus mutans*. Appl Environ Microbiol 77:8025–8033. <https://doi.org/10.1128/AEM.06362-11>.
24. Kino Y, Nakayama-Imaohji H, Fujita M, Tada A, Yoneda S, Murakami K, Hashimoto M, Hayashi T, Okazaki K, Kuwahara T. 2016. Counterselection employing mutated *pheS* for markerless genetic deletion in *Bacteroides* species. Anaerobe 42:81–88. <https://doi.org/10.1016/j.anaerobe.2016.09.004>.
 25. Zhou C, Shi L, Ye B, Feng H, Zhang J, Zhang R, Yan X. 2017. *pheS**, an effective host-genotype-independent counter-selectable marker for marker-free chromosome deletion in *Bacillus amyloliquefaciens*. Appl Microbiol Biotechnol 101:217–227. <https://doi.org/10.1007/s00253-016-7906-9>.
 26. Ward N, Larsen O, Sakwa J, Bruseth L, Khouri H, Durkin AS, Dimitrov G, Jiang LX, Scanlan D, Kang KH, Lewis M, Nelson KE, Methe B, Wu M, Heidelberg JF, Paulsen IT, Fouts D, Ravel J, Tettelin H, Ren QH, Read T, DeBoy RT, Seshadri R, Salzberg SL, Jensen HB, Birkeland NK, Nelson WC, Dodson RJ, Grindhaug SH, Holt I, Eidhammer I, Jonassen I, Vanaken S, Utterback T, Feldblyum TV, Fraser CM, Lillehaug JR, Eisen JA. 2004. Genomic insights into methanotrophy: the complete genome sequence of *Methylococcus capsulatus* (Bath). PLoS Biol 2:1616–1628. <https://doi.org/10.1371/journal.pbio.0020303>.
 27. Pol A, Barends TR, Dietl A, Khadem AF, Eygensteyn J, Jetten MS, Op den Camp HJ. 2014. Rare earth metals are essential for methanotrophic life in volcanic mudpots. Environ Microbiol 16:255–264. <https://doi.org/10.1111/1462-2920.12249>.
 28. Keltjens JT, Pol A, Reimann J, Op den Camp HJ. 2014. PQQ-dependent methanol dehydrogenases: rare-earth elements make a difference. Appl Microbiol Biotechnol 98:6163–6183. <https://doi.org/10.1007/s00253-014-5766-8>.
 29. Nakagawa T, Mitsui R, Tani A, Sasa K, Tashiro S, Iwama T, Hayakawa T, Kawai K. 2012. A catalytic role of XoxF1 as La³⁺-dependent methanol dehydrogenase in *Methylobacterium extorquens* strain AM1. PLoS One 7:e50480. <https://doi.org/10.1371/journal.pone.0050480>.
 30. Hibi Y, Asai K, Arafuka H, Hamajima M, Iwama T, Kawai K. 2011. Molecular structure of La³⁺-induced methanol dehydrogenase-like protein in *Methylobacterium radiotolerans*. J Biosci Bioeng 111:547–549. <https://doi.org/10.1016/j.jbiosc.2010.12.017>.
 31. Culpepper MA, Rosenzweig AC. 2014. Structure and protein-protein interactions of methanol dehydrogenase from *Methylococcus capsulatus* (Bath). Biochemistry 53:6211–6219. <https://doi.org/10.1021/bi500850j>.
 32. Larsen O, Karlsen OA. 2016. Transcriptomic profiling of *Methylococcus capsulatus* (Bath) during growth with two different methane monooxygenases. Microbiologyopen 5:254–267. <https://doi.org/10.1002/mbo3.324>.
 33. Kao WC, Chen YR, Yi EC, Lee H, Tian Q, Wu KM, Tsai SF, Yu SS, Chen YJ, Aebersold R, Chan SI. 2004. Quantitative proteomic analysis of metabolic regulation by copper ions in *Methylococcus capsulatus* (Bath). J Biol Chem 279:51554–51560. <https://doi.org/10.1074/jbc.M408013200>.
 34. Nielsen AK, Gerdes K, Murrell JC. 1997. Copper-dependent reciprocal transcriptional regulation of methane monooxygenase genes in *Methylococcus capsulatus* and *Methylosinus trichosporium*. Mol Microbiol 25:399–409. <https://doi.org/10.1046/j.1365-2958.1997.4801846.x>.
 35. Ve T, Mathisen K, Helland R, Karlsen OA, Fjellbirkeland A, Rohr AK, Andersson KK, Pedersen RB, Lillehaug JR, Jensen HB. 2012. The *Methylococcus capsulatus* (Bath) secreted protein, MopE*, binds both reduced and oxidized copper. PLoS One 7:e43146. <https://doi.org/10.1371/journal.pone.0043146>.
 36. Karlsen OA, Larsen O, Jensen HB. 2011. The copper responding surface of *Methylococcus capsulatus* Bath. FEMS Microbiol Lett 323:97–104. <https://doi.org/10.1111/j.1574-6968.2011.02365.x>.
 37. Karlsen OA, Kindingstad L, Angelskar SM, Bruseth LJ, Straume D, Puntervoll P, Fjellbirkeland A, Lillehaug JR, Jensen HB. 2005. Identification of a copper-repressible C-type heme protein of *Methylococcus capsulatus* (Bath): a member of a novel group of the bacterial di-heme cytochrome c peroxidase family of proteins. FEBS J 272:6324–6335. <https://doi.org/10.1111/j.1742-4658.2005.05020.x>.
 38. Karlsen OA, Lillehaug JR, Jensen HB. 2008. The presence of multiple c-type cytochromes at the surface of the methanotrophic bacterium *Methylococcus capsulatus* (Bath) is regulated by copper. Mol Microbiol 70:15–26. <https://doi.org/10.1111/j.1365-2958.2008.06380.x>.
 39. Kleiveland CR, Hult LT, Spetalen S, Kaldhusdal M, Christoffersen TE, Bengtsson O, Romarheim OH, Jacobsen M, Lea T. 2013. The noncommensal bacterium *Methylococcus capsulatus* (Bath) ameliorates dextran sulfate (sodium salt)-induced ulcerative colitis by influencing mechanisms essential for maintenance of the colonic barrier function. Appl Environ Microbiol 79:48–56. <https://doi.org/10.1128/AEM.02464-12>.
 40. Indrelid S, Kleiveland C, Holst R, Jacobsen M, Lea T. 2017. The soil bacterium *Methylococcus capsulatus* Bath interacts with human dendritic cells to modulate immune function. Front Microbiol 8:320. <https://doi.org/10.3389/fmicb.2017.00320>.
 41. Whittenbury R, Phillips KC, Wilkinson JF. 1970. Enrichment, isolation and some properties of methane-utilizing bacteria. J Gen Microbiol 61:205–218. <https://doi.org/10.1099/00221287-61-2-205>.
 42. Kato S, Goya E, Tanaka M, Kitagawa W, Kikuchi Y, Asano K, Kamagata Y. 2016. Enrichment and isolation of *Flavobacterium* strains with tolerance to high concentrations of cesium ion. Sci Rep 6:20041. <https://doi.org/10.1038/srep20041>.
 43. Ishikawa M, Tanaka Y, Suzuki R, Kimura K, Tanaka K, Kamiya K, Ito H, Kato S, Kamachi T, Hori K, Nakanishi S. 2017. Real-time monitoring of intracellular redox changes in *Methylococcus capsulatus* (Bath) for efficient bioconversion of methane to methanol. Bioresour Technol 241:1157–1161. <https://doi.org/10.1016/j.biortech.2017.05.107>.
 44. Newman JR, Fuqua C. 1999. Broad-host-range expression vectors that carry the L-arabinose-inducible *Escherichia coli* *araBAD* promoter and the *araC* regulator. Gene 227:197–203. [https://doi.org/10.1016/S0378-1119\(98\)00601-5](https://doi.org/10.1016/S0378-1119(98)00601-5).
 45. Quandt J, Hynes MF. 1993. Versatile suicide vectors which allow direct selection for gene replacement in Gram-negative bacteria. Gene 127:15–21. [https://doi.org/10.1016/0378-1119\(93\)90611-6](https://doi.org/10.1016/0378-1119(93)90611-6).
 46. Blodgett JA, Thomas PM, Li G, Velasquez JE, van der Donk WA, Kelleher NL, Metcalf WW. 2007. Unusual transformations in the biosynthesis of the antibiotic phosphinothricin tripeptide. Nat Chem Biol 3:480–485. <https://doi.org/10.1038/nchembio.2007.9>.